Available online at www.sciencedirect.com
ScienceDirect
Tetrahedron
Tetrahedron 63 (2007) 8761–8769

(*N*-7-Azaindolyl)oligothiophenes: synthesis, characterization, and photophysical properties

Jin Seok Hong,[a] Hyung Sup Shim,[a] Tae-Jeong Kim[a,*] and Youngjin Kang[b,*]

[a]*Department of Applied Chemistry, Kyungpook National University, 1370, Sankyug-Dong, Pook-Ku, Taegu 702-701, Republic of Korea*
[b]*Division of Science Education, Kangwon National University, Chun Cheon 200-701, Republic of Korea*

Received 17 May 2007; revised 12 June 2007; accepted 13 June 2007
Available online 16 June 2007

Abstract—The synthesis of a new series of mono- and oligothiophenes capped by 7-azaindoles such as 2-(*N*-azaindolyl)thiophene (**1**), 2-(*N*-azaindolyl)-5′-(bromo)oligothiophenes (**2a**–**4a**), and 2,5′-bis(*N*-azaindolyl)oligothiophenes (**2b**–**4b**) has been investigated. The reaction of 7-azaindole with 2-bromothiophene under the modified Ullmann condensation conditions led to the formation of **1**. Simple extension of the same method to the reaction of 2,5′-dibromooligothiophenes in the presence of 4–5 M excess of 7-azaindole led to the formation of **2a**–**4a** and **2b**–**4b** in moderate overall yields (40–55%). All compounds were fully characterized by analytical and various spectroscopic techniques. The structures of **2b**, **3b**, and **4b** were determined by X-ray diffraction analyses. All three compounds show several intermolecular C(π)···H interactions leading to the formation of herringbone packing in the solid-state structure. The UV absorption spectra of **1**–**4** consist of three characteristic electronic transitions corresponding to $n \rightarrow \pi^*$ and $\pi \rightarrow \pi^*$ transitions arising out of the π-conjugation of the entire molecule as well as local aromatic units. The emission spectra of the same compounds show intense fluorescence bands at the wavelengths between 422 and 495 nm. The length of the thiophene chain and the presence of bromine atom influence the band position of both absorption and emission spectra. While the extension in π-conjugation causes the reduction in the band gap, the bromine atom shifts the electronic transition energy to the blue region. The cyclic voltammetric measurements were performed with **1**–**4**, which show that the compounds exhibit a typical pseudo-reversible redox wave with E_{ox} in the range 0.6–1.2 V.

1. Introduction

Oligothiophenes with well-defined structures,[1] owing to their unique electronic and optical properties, are of great interest for new materials in several fields of applications such as field-effect transistors,[2] organic light-emitting diodes (OLEDs),[3] or photocopiers.[4] In addition, oligothiophenes have been reported to exhibit multiple redox processes, which are related to a stepwise formation of radical cations, dimerized radical cations (π-stacked radical cations), and dications. In principle, these different charge carriers can lead to paramagnetic or diamagnetic conducting materials through interchain transport.

Oligothiophenes with terminal groups bearing diarylamino functional groups have recently been used as efficient emitters[5] and reported to be potential hole-transporting materials.[6] The introduction of planar fluorene moieties as the end groups of bithiophene facilitates the π–π stacking of the crystals, resulting in the formation of new materials that exhibit extremely high field-effect mobility.[7] Various other groups have also been employed for the purpose of end capping the oligothiophenes. They are diarylboryl,[8] pyridyl,[9] diphenylphosphine,[10] and groups capable of charge transfer.[11]

In this regard, an *N*-donor chelated heterocyclic compound such as 7-azaindole deserves a special attention due to its application in OLEDs. Wang has demonstrated in a series of elegant publications that main group and transition metal complexes of 7-azaindolyl anion exhibit the blue luminescent property.[12] Although free 7-azaindole has no emission in the visible region in solution and a very weak in the solid state, the 7-azaindolyl anion exhibits a bright blue emission both in solution and in the solid state. However, those complexes incorporating 7-azaindolyl do not have a long-term stability in EL devices.[12d,13] Improved stability and the performance of OLEDs can be achieved by replacing the proton on the indole nitrogen atom by an aromatic group. When the 7-azaindolyl group is bound to benzene or biphenyl through nitrogen of the indolyl ring, a red shift from UV to blue is observed. At the same time, the thermal stability also increases significantly upon derivatization by aromatic moieties, some of which have shown promising results for application as a blue emitter and a hole transport material in OLEDs.[12f]

The present work is a result of our effort on the design of novel luminescent compounds for applications in OLEDs.[14]

* Corresponding authors. Tel.: +82 53 950 5587; fax: +82 53 950 6594; e-mail: tjkim@knu.ac.kr

0040–4020/$ - see front matter © 2007 Elsevier Ltd. All rights reserved.
doi:10.1016/j.tet.2007.06.037

We have investigated N-arylation of 7-azaindole with 1,1′-dibromooligothiophenes in an attempt to prepare a series of (7-azaindolyl)oligothiophenes as potential candidates for blue emitters and hole transport materials in OLEDs. Herein, we report their synthesis, structural characterization, photophysical, and electrochemical properties.

2. Results and discussion

2.1. Synthesis and characterization

Scheme 1 shows the routes leading to the formation of our target compounds **1**–**4**. All routes involve the extended Ullmann coupling reaction with a slight modification adopted by Buchwald.[15,16] Under the standard set of reaction conditions for the N-arylation of nitrogen heterocycles, the reaction of 2-bromothiophene with a slight molar excess of 7-azaindole led to the formation of 2-(*N*-7-azaindolyl)thiophene (**1**) in high yield (72%). Simple extension of the method to the reaction of 2,5′-dibromooligothiophenes in the presence of 4–5 M excess of 7-azaindole led indeed to the formation of mono- and bi-capped products, 2-(*N*-azaindolyl)-5′-(bromo)oligothiophenes (**2a**–**4a**) and 2,5′-bis(*N*-azaindolyl)oligothiophenes (**2b**–**4b**) in moderate overall yields (40–55%). Change of reaction conditions such as the ratio of reactants, the reaction time, and the reaction temperature had little effect on the product distribution as well as the overall yields. Sometimes repeated separation by column chromatography is necessary to obtain mono- and bi-capped products in a pure state. The compounds are stable in air/moisture in solution and in the solid state. These new compounds were fully characterized by elemental analyses and spectroscopic techniques.

2.2. X-ray crystal structures of 2b, 3b, and 4b

More definitive structural confirmation comes from X-ray crystallography in the cases of **2b**, **3b**, and **4b**. Their molecular structures are shown in Figures 1–3, and crystal data, bond distances, and angles collected in Tables 1 and 2. The bond lengths between the indolyl nitrogen atom and the α-carbon atoms of thiophene such as N2–C8, N1–C8, and N2–C8/N3–C19 in **2b**, **3b**, and **4b**, respectively, are in the region of 1.393(5)–1.4096(19) Å, which are comparable to those found in a related compound such as 1,3-bis(5,5′-*N*-7-azaindolyl-[2,2′]bithiophenyl-3-yl)-1,1,3,3-tetraphenyldisiloxane.[17] The most characteristic structural feature of **2b** is the presence of a two-fold axis of symmetry lying along the vector linking S1 and the midpoint of C9–C9A bond. Two azaindole substituents are oriented in a *syn* fashion making a pair of pyridyl nitrogen atoms and the sulfur atom point toward one another (Fig. 1). Such conformation is attributable to steric repulsion between N1 and C1–H.[10] The dihedral angle between 7-azaindole and thiophene rings in **2b** is approximately 30.92°, indicating the lack of effective π-conjugation. In contrast, however, two azaindole rings in both **3b** and **4b** are oriented in an *anti* fashion. This orientation can be due to the effective intermolecular interaction between two adjacent units. For examples, π-stacking in **4b** is observed between two 7-azaindole rings. The dihedral angle of two mean planes (C1–C4, C7, N1 and C4–C7, N2) is 1.14°, indicating that they are almost parallel to each other. The shortest distance (C1–C6) is 3.44 Å (see Supplementary data). Thiophene rings in both **3b** and **4b** are arranged in a nearly coplanar manner with *syn* and *syn*, *anti*-conformations for **3b** and **4b**, respectively (Figs. 2 and 3). Note that the dihedral angles between 7-azaindolde and thiophene rings in these compounds are quite small as compared to that of **2b**: 9.16° for **3b**; 9.32° and 12.57° for **4b**. These small dihedral angles are in good agreement with those found with oligophenylenes or oligothiophene.[18] Molecular coplanarity observed in **3b** and **4b**, unlike **2b**, makes the extended π-conjugation feasible throughout the whole molecule, which in turn has some implication in their photophysical properties (vide infra). Finally, in connection with a structural feature common to all three compounds, it is worth to note that they all exhibit various intermolecular interactions and herringbone packing leading to the formation of extended packing of the solid-state structure. Several intermolecular interactions, such as face-to-edge C(π)···H interactions, are observed in packing structure of all three compounds. As shown in Figure 3, **4b** exhibits intermolecular interaction between C2 and H1 with the separation distance of 2.80 Å. The dihedral angle of two mean planes (C1–C4, C7, N1) is 72.85°. Such observations support apparently that this interaction is face-to-edge C(π)···H interaction.[19] Details of C(π)···H interactions for other compounds are presented in Supplementary data. In general, π-stacking interactions in herringbone packing is one of the key factors that increase carrier mobility through the effective π-orbital overlap between two adjacent molecules.[20] In this respect, the effective π-stacking of herringbone packing observed with **4b** suggests that it is a potential candidate for use in organic semiconductor, which will be the topic of our future communication.

2.3. Thermal properties

The thermal properties of all new compounds were determined by TGA and DSC measurements (Table 3). They all show a decomposition temperature (T_{decomp}) higher than that of 7-azaindole (105 °C). As expected, thermal stability increases with increase in the numbers of the thiophene

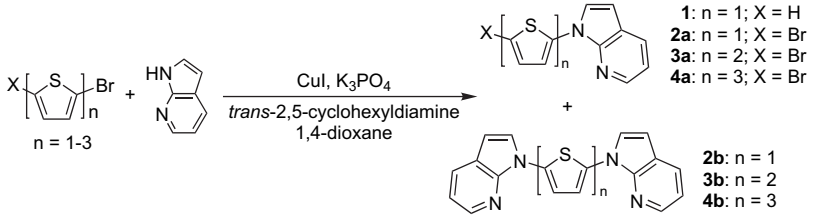

Scheme 1.

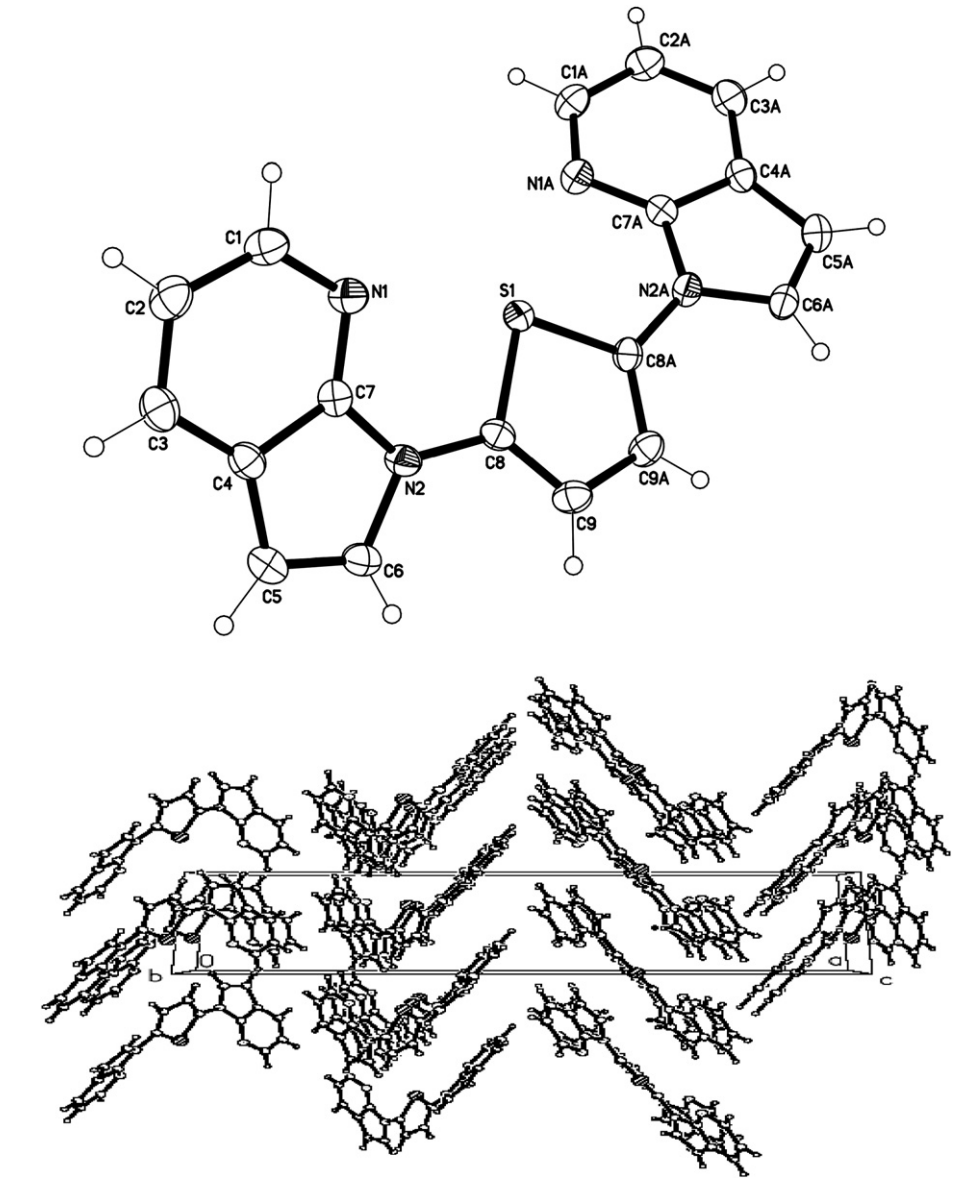

Figure 1. Top: the molecular structure of **2b** with atom labeling schemes and 50% thermal ellipsoids. Bottom: unit cell packing diagram of **2b**.

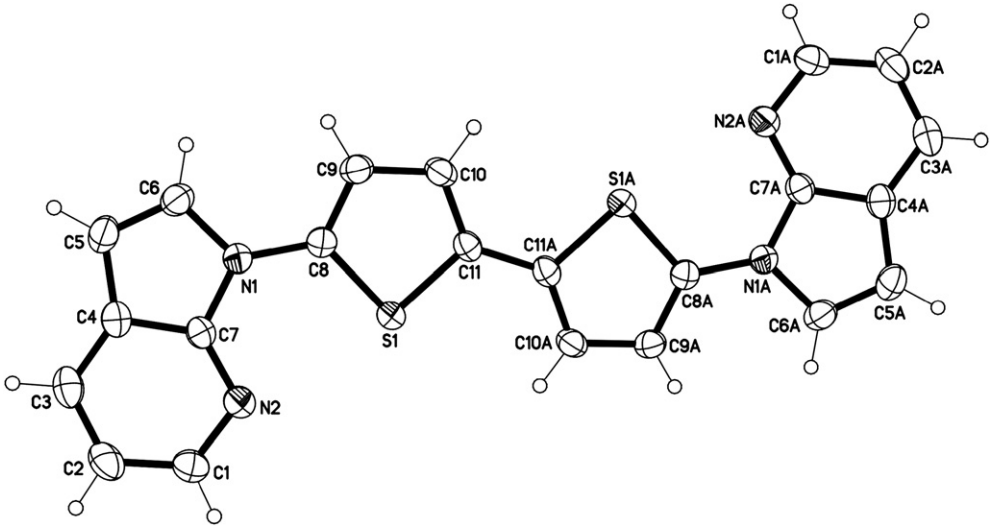

Figure 2. The molecular structure of **3b** with atom labeling schemes and 50% thermal ellipsoids.

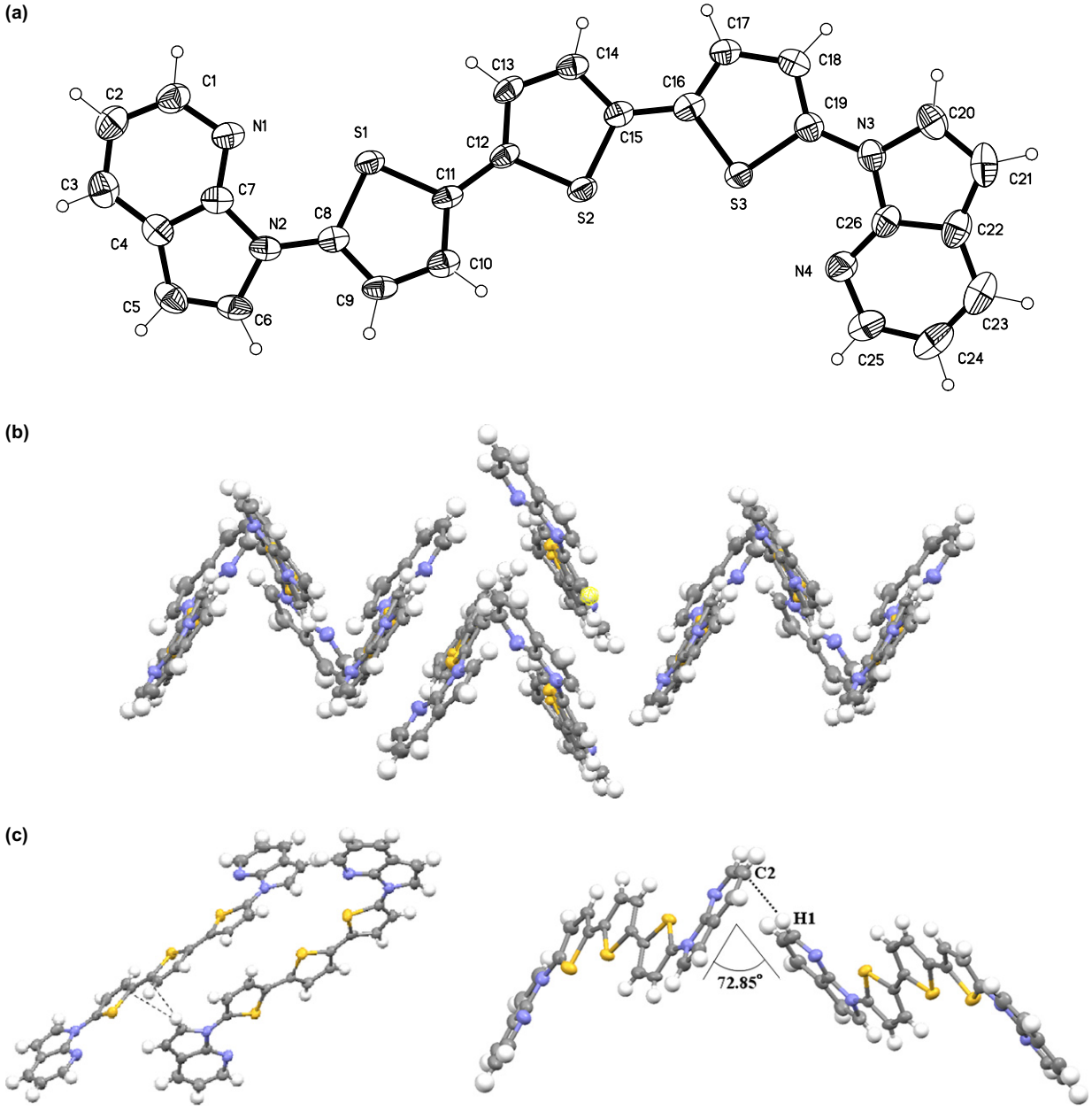

Figure 3. (a) The molecular structure of **4b** with atom labeling schemes and 50% thermal ellipsoids. (b) Packing diagram showing herringbone structure. (c) Diagram showing intermolecular C(π)···H interactions; C2–H1: 2.80 Å, C11–H6: 2.80 Å, C12–H6: 2.70 Å.

Table 1. Summary of crystallographic data for **2b**, **3b**, and **4b**

	2b	**3b**	**4b**
Formula	$C_{18}H_{12}N_4S$	$C_{22}H_{14}N_4S_2$	$C_{26}H_{16}N_4S_3$
MW	316.38	398.49	480.61
T/K	173(2)	173(2)	173(2)
Crystal system	Trigonal	Monoclinic	Monoclinic
Space group	$P3_121$	$P2_1/c$	$P2_1/c$
Unit cell dimension	a=7.05505(3) Å, α=90°	a=10.8458(9) Å, α=90°	a=28.2102(2) Å, α=90°
	b=7.0505(3) Å, β=90°	b=6.1379(5) Å, β=91.511(2)°	b=5.8342(5) Å, β=96.588(2)°
	c=25.151(3) Å, γ=120°	c=13.4651(11) Å, γ=90°	c=13.1903(11) Å, γ=90°
V/Å^3	1082.74(13)	896.07(13)	2156.5(3)
Z	3	2	4
μ(Mo Kα)/mm^{-1}	0.229	0.313	0.368
Crystal size/mm^3	0.60×0.40×0.40	0.60×0.25×0.08	0.35×0.30×0.04
Reflections collected	6981	5444	12,638
Independent reflections	1747 [R(int)=0.0394]	2095 [R(int)=0.0335]	4988 [R(int)=0.0820]
Goodness-of-fit on F^2	1.140	1.065	1.092
Final $R1$, $wR2$ [$I>2\sigma(I)$]	0.0321, 0.0858	0.0350, 0.0884	0.0577, 0.1362
R indices (all data)	0.0335, 0.0868	0.0473, 0.0958	0.1425, 0.1744

Table 2. Selected bond lengths (Å) and angles (°) for **2b**, **3b**, and **4b**

Compound **2b**			
N2–C8	1.4096(19)	S1–C8	1.7407(14)
N2–C6	1.3973(19)	C9–C9A[a]	1.422(3)
N2–C8–S1	120.26(11)	N2–C8–C9	126.85(13)
C7–N2–C8	127.91(12)	C6–N2–C8	124.24(13)
Compound **3b**			
C11–C11A[b]	1.456(3)	N1–C8	1.408(2)
S1–C8–N1	121.27(12)	C6–N1–C8	124.76(14)
C10–C11–C11A[b]	129.31(19)	S1–C11–C11A[b]	111.29(12)
Compound **4b**			
N2–C8	1.403(5)	C11–C12	1.419(6)
C15–C16	1.402(7)	C19–N3	1.393(5)
C7–N2–C8	127.2(3)	S1–C11–C12	119.6(3)
C14–C15–C16	128.5(4)	C15–C16–S3	119.9(3)
S3–C19–N3	120.7(3)		

[a] $y, x, -z$.
[b] $-x+1, -y, -z+1$.

unit in the following order of T_{decomp}: **1**<**2a**<**4a**<**3a** and **1**<**2b**<**3b**<**4b**. When the comparison is made between mono- and bi-capped products in the same homologue, those belonging to the latter are thermally more stable than those belonging to the former. These results support the observation that as the number of thiophene rings increases the molecules tend to give crystalline forms due to the formation of an undisturbed π-conjugation system. In fact, the compounds **2b**–**4b** showed no weight loss below 355 °C and only 10% loss in the temperature range 355–393 °C. The compound **4b** with the longest thiophene chain exhibits the highest T_{decomp} (394 °C) of all. The glass transition temperatures (T_g), however, seem to be independent of the chain length as shown in Table 3. The table also shows that thermally more stable series (**2b**–**4b**) exhibit even lower T_g values (65–67 °C) than their less stable counterparts **2a**–**4a** (102–116 °C). Obviously some sort of intermolecular interactions, in addition to the chain length contribution, may be operating in the solid state. These observations are contrary to those noted earlier in connection with related compounds.[12f]

2.4. Photophysical properties

The UV absorption spectra of **2**–**4** taken in CH_2Cl_2 are shown in Figures 4 and 5, with the λ_{max} values of **1**–**4** and 7-azaindole collected in Table 3. 7-Azaindole exhibits a pair of characteristic absorption bands at 237 and 282 nm, assignable to the $\pi\rightarrow\pi^*$ transition and the $n\rightarrow\pi^*$ transition, respectively. The absorption spectra of all new compounds

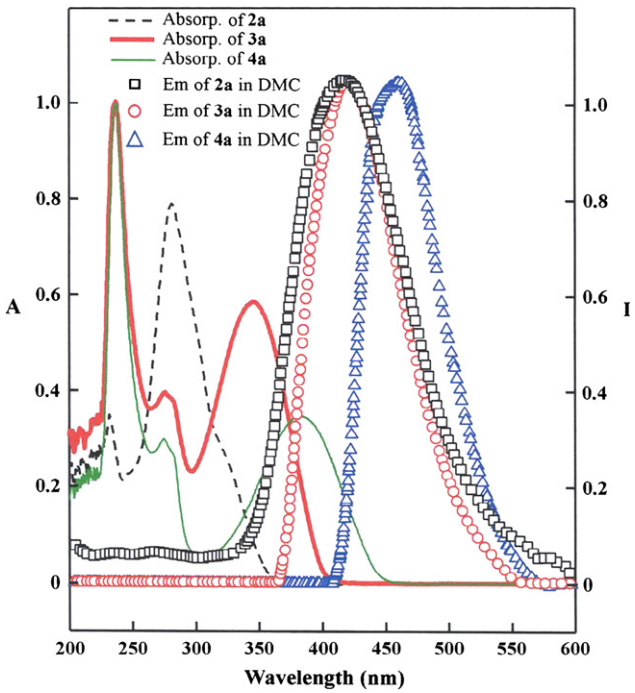

Figure 4. Absorption and emission spectra of **2a**, **3a**, and **4a** in DMC.

consist of three electronic transitions with the strongest absorption band at longer wavelengths assignable to $\pi\rightarrow\pi^*$ transition of the entire conjugated backbone while the less intense one (near 273–282 nm) being assignable to the $\pi\rightarrow\pi^*$ transition centered at the local aromatic units. The absorption at the shortest wavelengths (231–237 nm) is attributable to the $n\rightarrow\pi^*$ of the thiophene unit. N-Arylation of 7-azaindole with bromothiophene results in a red shift for these azaindole-centered transitions along with the appearance of an additional band due to the presence of thiophene moiety. The length of the thiophene chain obviously plays a role to show the following trend in λ_{max}: **2a** (320 nm)<**3a** (346 nm)<**4a** (383 nm) (Fig. 4). The presence of a bromine atom found in **2a**–**4a** shifts the absorption energy to the blue region when compared with bi-capped series (**2b**–**4b**) as shown in Table 3 (vide infra).

The emission spectra of the same compounds taken in CH_2Cl_2 are also shown in Figures 4 and 5, with their λ_{max} values collected in Table 3. As known elsewhere, the anion of 7-azaindole after the removal of indole proton exhibits a bright blue emission in solution and the solid state.

Table 3. Photophysical and electrochemical data for 7-azaindole and **1**–**4**

Compd	T_g (°C)	T_{decomp} (°C)	UV[a] λ_{max} (nm)	PL[a] λ_{max} (nm)	Φ_{fl}[b] (%)	$E_{ox}(\{E_{ONSET}\}^{ox})$ V versus SCE	E_g[c] (eV)	HOMO/LUMO (eV)
7-Azaindole	—	—	237, 282	347	—	—	—	—
1	76	197	231, 273, 315	422	1.8	1.14 (1.05)	3.58	−5.77/−2.19
2a	102	202	230, 279, 320	428	5.8	1.17 (1.08)	3.51	−5.79/−2.29
3a	105	263	237, 276, 346	423	7.9	0.94 (0.76)	3.13	−5.48/−2.35
4a	116	238	237, 275, 383	468	7.1	0.88, 1.20 (0.73)	2.83	−5.45/−2.62
2b	66	356	236, 282, 319	460, 493	3.2	0.89, 1.19 (0.77)	3.34	−5.49/−2.15
3b	65	382	236, 275, 363	429, 450	11	0.65, 0.96 (0.54)	2.97	−5.26/−2.29
4b	67	394	237, 274, 396	465, 495	10	0.62, 0.87, 1.13 (0.5)	2.70	−5.23/−2.53

[a] Measured in CH_2Cl_2.
[b] Determined by the dilute method.
[c] Calculated by optical edge.

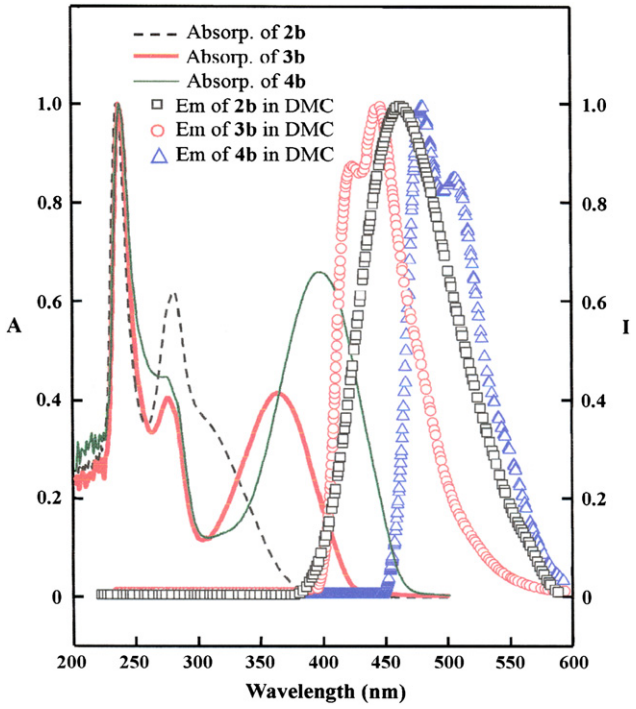

Figure 5. Absorption and emission spectra of **2b**, **3b**, and **4b** in DMC.

Similarly, all the compounds show intense fluorescence emission at the wavelengths between 422 and 495 nm in the following order of emission maxima: **1**<**3a**<**2a**<**4a** and **1**<**3b**<**2b**<**4b**. The conjugation of 7-azaindolyl ring with oligothiophene causes a red shift in emission energy by decreasing the $\pi\rightarrow\pi^*$ gap in **1**–**4**.[13] Compound **1** emits at the shortest wavelength (422 nm) than any of the rest. The presence of a bromine atom in **2a**–**4a** appears to lower the band gap and shift the emission energy to the blue region as compared with the emission maxima for **2b**–**4b**. The most striking difference in the emission pattern between the mono-capped series (**2a**–**4a**) and bi-capped ones (**2b**–**4b**) is that the former exhibits single emission maxima, while the latter shows additional ones at a little longer wavelengths (Table 3), probably due to phosphorescence.[12g]

Table 3 summarizes the oxidation potentials of **1**–**4** versus standard calomel electrode (SCE) as obtained from the cyclic voltammetric (CV) measurements. Typical pseudo-reversible redox waves were observed in the positive potential region with E_{ox} in the range 0.6–1.2 V.[21] The oxidation potential, as expected, is a function of the numbers of thiophene: namely, it decreases with the increase in chain length due to extension in π-conjugation. In this regard, it is understandable that **1** and **2a** exhibit the highest oxidation potentials than others in the whole series. When the comparison is made between **1** and **2a**, even higher oxidation potential with **2a** (by 30 mV) can be noted. This observation in connection with the bromine atom in **2a**–**4a** is consistent with the blue shift found in their absorption spectra. Another interesting feature in connection with oxidation potential is that more than one oxidation process is taking place in **4a** and **2b**–**4b**: two stepwise oxidations in **4a**, **2b**, and **3b**, and three successive oxidations in **4b**. A typical CV of **3b** is shown in Figure 6 showing the redox waves in the positive potential region.

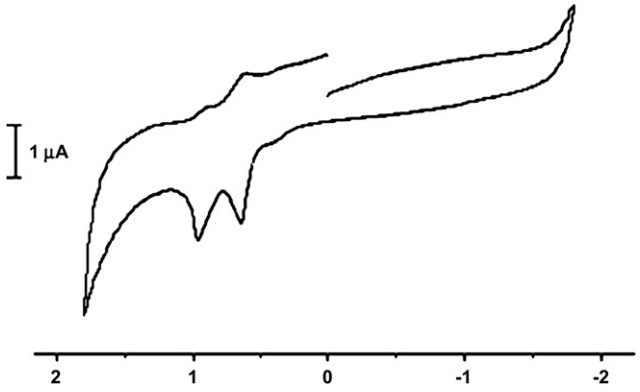

Figure 6. Cyclic voltammogram of **3b**.

The HOMO energy levels of **1**–**4** are calculated from the onset of oxidation potential according to the equation IP (ionization potential)=$\{(E_{ONSET})^{ox}+4.4\}$V,[22] and the LUMO energy level is obtained by the subtraction of the optical band gap from the IP (Table 3). Here again, it is not surprising to note consistency inherent in the trend in the HOMO level as well as the HOMO/LUMO gap. Namely, they are the function of not only substitution but also the numbers of thiophene. For instance, a more electronegative bromine atom is capable of lowering the HOMO level and increasing the HOMO/LUMO gap. As for the band gap, a reduction is maintained as the number of thiophene increases.

3. Conclusions

The reaction of 1,1′-dibromooligothiophenes in the presence of a 4–5 M excess of 7-azaindole led to the formation of mono- and bi-capped products, 2-(*N*-azaindolyl)-5′-(bromo)oligothiophenes (**2a**–**4a**) and 2,5′-bis(*N*-azaindolyl)-oligothiophenes (**2b**–**4b**) in moderate overall yields (40–55%). These new compounds were fully characterized by NMR, mass spectroscopy, elemental analyses, and X-ray crystallography (in the case of **2b**–**4b**). All three compounds show several intermolecular C(π)···H interactions leading to the formation of herringbone packing in the solid-state structure. The UV absorption spectra of **1**–**4** consist of three characteristic $n\rightarrow\pi^*$ and $\pi\rightarrow\pi^*$ electronic transitions, which are attributable to the π-conjugation of the entire molecule as well as local aromatic units. The emission spectra of the same compounds show intense fluorescence bands between 422 and 495 nm. All the compounds exhibit pseudo-reversible cyclic voltammograms with positive redox potentials. The HOMO/LUMO energy levels are found to be influenced by the number of thiophenes and the presence of bromine.

4. Experimental section

4.1. General remarks

All reactions were carried out under an atmosphere of nitrogen using standard Schlenk techniques. Solvents were dried using standard procedures. The ^{1}H and ^{13}C NMR experiments were performed on a Bruker Advance 400 or 500

spectrometer by Korea Basic Science Institute (KBSI). Chemical shifts were given as δ values with reference to tetramethylsilane (TMS) as an internal standard. Coupling constants are in Hertz. IR spectra were run on a Mattson FTIR Galaxy 6030E spectrophotometer by KBSI. Elemental analyses were performed by Center for Instrumental Analysis, Kyungpook National University. UV/vis and photoluminescent spectra for all samples with concentrations in the range of 10–50 μM in CH_2Cl_2 were obtained with a Lambda 900 UV/vis spectrometer and a Perkin–Elmer Luminescence spectrometer LS 50B. All solutions for photophysical experiments were degassed with more than three repeated freeze–pump–thaw cycles in a vacuum line. Cyclic voltammetry was performed with an Autolab potentiostat from Echochemie under nitrogen in a one-compartment electrolysis cell consisting of a platinum wire working electrode, a platinum wire counter electrode, and a quasi Ag/AgCl reference electrode. Cyclic voltammograms were monitored at scan rates of either 100 or 50 mV s^{-1} and recorded in acetonitrile. The concentration of the complex was maintained at 0.5 mM or less and each solution contained 0.1 M of tetrabutylammonium perchloride (TBAP) as the electrolyte. The ferrocenium/ferrocene couple (0.40 V) was used as an internal standard. All commercial reagents were purchased from Aldrich and used as received. 5,5′-Dibromobithiophene and 5,5′-dibromo-2,2′:5′,2″-terthiophene were prepared as reported earlier.[23]

4.2. 2-(*N*-Azaindolyl)thiophene (1)

A Schlenk tube charged with CuI (11.70 mg, 0.06 mmol, 1.0 mol %), 7-azaindole (0.87 g, 7.36 mmol), and K_3PO_4 (2.62 g, 12.26 mmol) was evacuated twice and back-filled with nitrogen. 2-Bromothiophene (1.40 mL, 6.13 mmol), *trans*-1,2-cyclohexanediamine (74.0 μL, 0.61 mmol, 10 mol %), and dioxane (8.0 mL) were then successively added under nitrogen. The Schlenk tube was then sealed and the reaction mixture stirred with heating in an oil bath at 110 °C for 24 h. The tube was cooled to ambient temperature, open to air, the reaction mixture diluted with dichloromethane (3 mL), and filtered through a Celite bed. Column chromatography (hexane/ethyl acetate, 9:1 v/v) after usual workups afforded the product as an off-white solid. Yield: 0.88 g (72%). ^{1}H NMR ($CDCl_3$): δ 6.59 (1H, d, ^3J=3.6), 7.02 (1H, dd, $^3J_1$=9.1, $^3J_2$=1.8), 7.11 (1H, s), 7.13 (1H, dd, $^3J_1$=7.8, $^3J_2$=2.1), 7.25 (1H, dd, $^3J_1$=10.1, $^3J_2$=5.9), 7.48 (1H, d, ^3J=3.7), 7.92 (1H, dd, $^3J_1$=9.3, $^3J_2$=6.2), 8.41 (1H, dd, $^3J_1$=6.3, $^3J_2$=3.3). Anal. Calcd for $C_{11}H_8N_2S_1$: C, 65.97; H, 4.03; N, 13.99; S, 16.01. Found: C, 66.02; H, 4.00; N, 14.13; S, 15.67.

4.3. 2-(5-Bromothiophenyl)-1-(7-azaindole) (2a) and 2,5-bis(1-(7-azaindolyl))thiophene (2b)

A Schlenk tube charged with CuI (18.30 mg, 0.10 mmol, 1.0 mol %), 7-azaindole (1.13 g, 9.60 mmol), and K_3PO_4 (4.19 g, 19.20 mmol) was evacuated twice and back-filled with nitrogen. 2,5-Dibromothiophene (0.50 mL, 4.80 mmol), *trans*-1,2-cyclohexanediamine (115 μL, 0.96 mmol, 10 mol %), and dioxane (6.0 mL) were then successively added under nitrogen. The tube was sealed and the reaction mixture stirred with heating in an oil bath at 110 °C for 24 h. The tube was cooled to ambient temperature, open to air, the reaction mixture diluted with dichloromethane (3 mL), and filtered through a Celite bed. The resulting solution was evaporated to dryness under reduced pressure and the residue redissolved in dichloromethane (3 mL) to be charged in a silica gel column. Two bands eluted with a mixture of hexane and ethyl acetate (9:1, v/v) were collected successively. The compound **2a** was eluted out first followed by the compound **2b**.

Compound **2a** (first band): isolated as a pale pink solid. Yield: 0.28 g (23%). ^{1}H NMR ($CDCl_3$): δ 6.62 (1H, d, ^3J=3.6), 6.96 (1H, d, ^3J=3.9), 7.00 (1H, d, ^3J=4.2), 7.16 (1H, dd, $^3J_1$=11.7, $^3J_2$=3.0), 7.46 (1H, d, ^3J=3.6), 7.95 (1H, dd, $^3J_1$=9.3, $^3J_2$=6.6), 8.41 (1H, dd, $^3J_1$=6.0, $^3J_2$=3.3). Anal. Calcd for $C_{10}H_8N_2SBr$: C, 47.33; H, 2.53; N, 10.04; S, 11.49. Found: C, 47.38; H, 2.47; N, 10.05; S, 11.24.

Compound **2b** (second band): isolated as a pale pink solid. Yield: 0.22 g (18%). ^{1}H NMR ($CDCl_3$): δ 6.64 (2H, d, ^3J=3.6), 7.16 (2H, dd, $^3J_1$=12.6, $^3J_2$=3.3), 7.19 (2H, s), 7.54 (2H, d, ^3J=3.6), 7.96 (2H, dd, $^3J_1$=9.3, $^3J_2$=6.3), 8.41 (2H, dd, $^3J_1$=5.7, $^3J_2$=3.3). Anal. Calcd for $C_{18}H_{12}N_4S$: C, 68.33; H, 3.82; N, 17.71; S, 10.13. Found: C, 68.21; H, 3.85; N, 17.81; S, 9.99.

4.4. 5′-(5-Bromo-2,2′-bithiophenyl)-1-(7-azaindole) (3a) and 5,5′-bis(1-(7-azaindolyl))-2,2′-bithiophene (3b)

A Schlenk tube charged with CuI (0.02 g, 0.12 mmol, 1.0 mol %), 7-azaindole (2.20 g, 18.60 mmol), and K_3PO_4 (5.24 g, 24.70 mmol) was evacuated twice and back-filled with nitrogen. 5,5′-Dibromo-2,2′-bithiophene (2.0 g, 6.17 mmol), *trans*-1,2-cyclohexanediamine (224 μL, 1.86 mmol, 10 mol %), and dioxane (8.0 mL) were then successively added under nitrogen. The tube was sealed and the reaction mixture was stirred with heating in an oil bath at 110 °C for 24 h. The tube was cooled to ambient temperature, open to air, the reaction mixture diluted with dichloromethane (3 mL), and filtered through a Celite bed. The resulting solution was evaporated to dryness under reduced pressure and the residue redissolved in dichloromethane (3 mL) to be charged in a silica gel column. Two bands eluted with a mixture of hexane and ethyl acetate (9:1, v/v) were collected successively.

Compound **3a** (first band): isolated as a yellow solid. Yield: 0.69 g (31%). ^{1}H NMR ($CDCl_3$): δ 6.64 (1H, d, ^3J=3.6), 6.93 (1H, d, ^3J=3.9), 6.98 (1H, d, ^3J=3.9), 7.03 (1H, d, ^3J=3.9), 7.15 (1H, d, ^3J=3.9), 7.18 (1H, dd, $^3J_1$=5.6, $^3J_2$=3.2), 7.52 (1H, d, ^3J=3.6), 7.96 (1H, dd, $^3J_1$=9.4, $^3J_2$=6.4), 8.44 (1H, dd, $^3J_1$=6.3, $^3J_2$=3.1). Anal. Calcd for $C_{15}H_9N_2S_2Br$: C, 49.87; H, 2.51; N, 7.75; S, 17.75. Found: C, 49.62; H, 2.55; N, 7.84; S, 17.99.

Compound **3b** (second band): isolated as a pale yellow solid. Yield: 0.53 g (24%). ^{1}H NMR ($CDCl_3$): δ 6.65 (2H, d, ^3J=3.6), 7.12 (2H, d, ^3J=3.9), 7.16–7.20 (4H, m), 7.54 (2H, d, ^3J=3.6), 7.97 (2H, dd, $^3J_1$=9.3, $^3J_2$=6.3), 8.45 (2H, dd, $^3J_1$=6.3, $^3J_2$=3.0). Anal. Calcd for $C_{22}H_{14}N_4S_2$: C, 66.31; H, 3.54; N, 14.06; S, 16.09. Found: C, 68.21; H, 3.85; N, 17.81; S, 15.82.

4.5. 5″-(5-Bromo-2,2′:5′,2″-terthiophenyl)-1-(7-azaindole) (4a) and 5,5″-bis(1-(7-azaindole))-2,2′:5′,2″-terthiophene (4b)

A Schlenk tube charged with CuI (11.80 mg, 0.06 mmol, 1.0 mol %), 7-azaindole (1.10 g, 9.27 mmol), and K_3PO_4 (2.62 g, 12.30 mmol) was evacuated twice and backfilled with nitrogen. 5,5″-Dibromo-2,2′:5′,2″-terthiophene (1.25 g, 3.09 mmol), *trans*-1,2-cyclohexanediamine (112 μL, 0.93 mmol, 10 mol %), and dioxane (6.0 mL) were then successively added under nitrogen. The tube was sealed and the reaction mixture was stirred with heating in an oil bath at 110 °C for 24 h. The tube was cooled to ambient temperature, open to air, the reaction mixture diluted with dichloromethane (3 mL), and filtered through a Celite bed. The resulting solution was evaporated to dryness under reduced pressure and the residue redissolved in dichloromethane (3 mL) to be charged in a silica gel column. Two bands eluted with a mixture of hexane and ethyl acetate (9:1, v/v) were collected successively.

Compound **4a** (first band): isolated as a yellow solid. Yield: 0.34 g (25%). ^{1}H NMR ($CDCl_3$): δ 6.65 (1H, d, ^3J=3.6), 6.92 (1H, d, ^3J=3.5), 6.98 (1H, d, ^3J=4.0), 7.03 (1H, d, ^3J=3.5), 7.09 (1H, d, ^3J=3.5), 7.10 (1H, s), 7.18 (1H, d, ^3J=1.5), 7.19 (1H, d, ^3J=1.0), 7.96 (1H, dd, $^3J_1$=9.2, $^3J_2$=6.2), 8.45 (1H, dd, $^3J_1$=6.2, $^3J_2$=3.3). Anal. Calcd for $C_{19}H_{11}N_2S_3Br$: C, 51.47; H, 2.50; N, 6.32; S, 21.69. Found: C, 51.66; H, 2.68; N, 6.34; S, 21.55.

Compound **4b** (second band): isolated as a pale yellow solid. Yield: 0.29 g (20%). ^{1}H NMR ($CDCl_3$): δ 6.58 (2H, d, ^3J=3.7), 7.03 (2H, d, ^3J=3.3), 7.05 (2H, d, ^3J=3.0), 7.09–7.13 (4H, m), 7.47 (2H, d, ^3J=3.6), 7.90 (2H, dd, $^3J_1$=9.1, $^3J_2$=6.5), 8.38 (2H, dd, $^3J_1$=5.9, $^3J_2$=3.3). Anal. Calcd for $C_{26}H_{16}N_4S_3$: C, 64.97; H, 3.35; N, 11.66; S, 20.01. Found: C, 65.12; H, 3.51; N, 11.91; S, 19.69.

4.6. X-ray crystallographic analyses

Single crystals of **2b**, **3b**, and **4b** suitable for X-ray diffraction analyses were obtained by slow diffusion of hexane into a dichloromethane solution containing each compound. The crystals of **2b**, **3b**, and **4b** were attached to glass fibers and mounted on a Bruker SMART diffractometer equipped with graphite monochromated Mo Kα (λ=0.71073 Å) radiation, operating at 50 kV and 30 mA, and a CCD detector; 45 frames of two-dimensional diffraction images were collected and processed to obtain the cell parameters and orientation matrix. All data collections were performed at 173 K. The data collection 2θ ranges for **2b**, **3b**, and **4b** are 4.86–56.5, 3.76–56.44, and 2.9–56.5, respectively. The first 50 frames were retaken after complete data collection and compared. The crystals showed no significant decay and no corrections were applied for the decay. The raw data were processed to give structure factors using the SAINT program.[24] Each structure was solved by direct methods and refined by full matrix least squares against F^2 for all data using SHELXTL software (version 5.10).[25] All non-hydrogen atoms in compounds **2b**, **3b**, and **4b** were anisotropically refined. All hydrogen atoms were placed in idealized positions and refined using a riding model. The crystal system in compound **2b** belongs to the trigonal $P3_121$ space group. The crystal system in both **3b** and **4b** belongs to the monoclinic $P2_1/c$, space group. Crystal data for **2b**, **3b**, and **4b** are summarized in Table 1. The refined atomic coordinates and anisotropic thermal parameters are included in electronic supplementary data. Crystallographic data for the structure reported here have been deposited with the Cambridge Crystallographic Data Centre (Deposition no. CCDC-646595 for **2b**, CCDC-646596 for **3b**, CCDC-646597 for **4b**). The data can be obtained free of charge via http://www.ccdc.cam.ac.uk./perl/catreq/catreq.cgi (or from the CCDC, 12 Union Road, Cambridge CB2 1EZ, UK; fax: +44 1223 336033; e-mail: deposit@ccdc.cam.ac.uk).

Acknowledgements

This work was supported by a grant from The Advanced Medical Technology Cluster for Diagnosis and Prediction at KNU from MOCIE, ROK. We thank Dr. Pattubala A. N. Reddy, KNU for helpful discussion.

Supplementary data

Tables giving atomic coordinates, displacement parameters, bond distances and angles, and packing diagrams for **2b**, **3b**, and **4b** are provided. Supplementary data associated with this article can be found in the online version, at doi:10.1016/j.tet.2007.06.037.

References and notes

1. Fichou, D. *Handbook of Oligo- and Polythiophenes*; Wiley-VCH: Weinheim, 1999.
2. Horowitz, G.; Garnier, F.; Yassar, A.; Hajlaoui, R.; Kouki, F. *Adv. Mater.* **1996**, *8*, 52.
3. (a) Rothberg, L. J.; Lovinger, A. J. *J. Mater. Res.* **1996**, *11*, 3174; (b) Justel, T.; Nikol, H.; Ronda, C. *Angew. Chem.* **1998**, *110*, 3251; *Angew. Chem., Int. Ed.* **1998**, *37*, 3084.
4. (a) Wurthner, F.; Yao, S.; Schilling, J.; Wortmann, R.; Redi-Abshiro, M.; Mecher, E.; Gallego-Gomez, F.; Meerholz, K. *J. Am. Chem. Soc.* **2001**, *123*, 2810; (b) Keil, D.; Flaig, R.; Schroeder, A.; Hartmann, H. *Dyes Pigment* **2001**, *50*, 67.
5. Noda, T.; Ogawa, H.; Noma, N.; Shirota, Y. *J. Mater. Chem.* **1999**, *9*, 2177.
6. (a) Kisselev, R.; Thelakkat, M. *Chem. Commun.* **2002**, 1530; (b) Wong, K.-T.; Hung, T. H.; Kao, S. C.; Chou, C. H.; Su, Y. O. *Chem. Commun.* **2001**, 1628; (c) Hartmann, H.; Gerstner, P.; Rohde, D. *Org. Lett.* **2001**, *3*, 1673; (d) Noda, T.; Ogawa, H.; Noma, N.; Shirota, Y. *Adv. Mater.* **1999**, *9*, 720; (e) Noda, T.; Imae, I.; Noma, N.; Shirota, Y. *Adv. Mater.* **1999**, *9*, 239.
7. Meng, H.; Bao, Z.; Lovinger, A. J.; Wang, B.-C.; Mujsce, A. M. *J. Am. Chem. Soc.* **2001**, *123*, 9214.
8. Noda, T.; Shirota, Y. *J. Am. Chem. Soc.* **1998**, *120*, 9714.
9. Hock, J.; Cargill Thompson, A. M. W.; McCleverty, J. A.; Ward, M. D. *J. Chem. Soc., Dalton Trans.* **1996**, 4257.
10. Field, J. S.; Haines, R. J.; Lakoba, E. I.; Sosabowski, M. H. *J. Chem. Soc., Perkin Trans. 1* **2001**, 3352.
11. (a) Apperloo, J. J.; Langeveld-Voss, B. M. W.; Knol, J.; Hummelen, J. C.; Janssen, R. A. J. *Adv. Mater.* **2000**, *12*, 908; (b) Wurthner, F.; Vollmer, M. S.; Effenberger, F.; Emele,

P.; Meyer, D. U.; Port, H.; Wolf, H. C. *J. Am. Chem. Soc.* **1995**, *117*, 8090.

12. (a) Hassan, A.; Breeze, S. R.; Courtenay, S.; Deslippe, C.; Wang, S. *Organometallics* **1996**, *15*, 5613; (b) Ashenhurst, J.; Wu, G.; Wang, S. *J. Am. Chem. Soc.* **2000**, *122*, 2541; (c) Wu, Q.; Lavigne, J. A.; Tao, Y.; D'Iorio, M.; Wang, S. *Inorg. Chem.* **2000**, *39*, 5248; (d) Liu, S.-F.; Wu, Q.; Schmider, H. L.; Aziz, H.; Hu, N.-X.; Popovic, Z.; Wang, S. *J. Am. Chem. Soc.* **2000**, *122*, 3671; (e) Wang, S. *Coord. Chem. Rev.* **2001**, *215*, 79; (f) Wu, Q.; Lavigne, J. A.; Tao, Y.; D'Iorio, M.; Wang, S. *Chem. Mater.* **2001**, *13*, 71; (g) Kang, Y.; Song, D.; Schmider, H.; Wang, S. *Organometallics* **2002**, *21*, 2413; (h) Kang, Y.; Wang, S. *Tetrahedron Lett.* **2002**, *43*, 3711; (i) Jia, W.-L.; Liu, Q.-D.; Wang, R.; Wang, S. *Organometallics* **2003**, *22*, 4070; (j) Lee, J.; Liu, Q.-D.; Motala, M.; Dane, J.; Gao, J.; Kang, Y.; Wang, S. *Chem. Mater.* **2004**, *16*, 1869; (k) Jia, W.-L.; Bai, D.-R.; McCormick, T.; Liu, Q.-D.; Motala, M.; Wang, R.-Y.; Seward, C.; Tao, Y.; Wang, S. *Chem.—Eur. J.* **2004**, *10*, 994.
13. (a) Wu, Q.; Esteghamatian, M.; Hu, N. X.; Popovic, Z.; Enright, G.; Breeze, S. R.; Wang, S. *Angew. Chem., Int. Ed.* **1999**, *38*, 985; (b) Hassan, A.; Wang, S. *Chem. Commun.* **1998**, 211; (c) Liu, W.; Hassan, A.; Wang, S. *Organometallics* **1997**, *16*, 4257; (d) Ashenhurst, J.; Brancaleon, L.; Hassan, A.; Liu, W.; Schmider, H.; Wang, S.; Wu, Q. *Organometallics* **1998**, *17*, 3186.
14. (a) Lee, E. J.; Hong, J. S.; Kim, T.-J.; Kang, Y.; Han, E. M.; Lee, J. J.; Song, K.; Kim, D.-U. *Bull. Korean Chem.* **2005**, *26*, 1946; (b) Kim, T.-J.; Kim, D.-U.; Paik, S.-H.; Kim, S.-H.; Tak, S.-H.; Han, Y.-S.; Kim, K.-B.; Ju, H.-J. *Mater. Sci. Eng. C* **2004**, *24*, 147; (c) Kim, K.-D.; Han, Y.-S.; Tak, Y.-H.; Kim, D.-U.; Kim, T.-J.; Yoon, U.-C.; Kim, S.-H.; Moon, H.-W. European Patent No. 03027185.2 (EU), 2004, 01. 20.
15. Hassan, J.; Sevignon, M.; Gozzi, C.; Schulz, E.; Lemaire, M. *Chem. Rev.* **2002**, *102*, 1359.
16. Klapars, A.; Antilla, J. C.; Huang, X.; Buchwald, S. L. *J. Am. Chem. Soc.* **2001**, *123*, 7727.
17. Song, K.-H.; Lee, T.; Jung, I.; Kang, Y.; Lee, H. I.-S.; Kang, S.-J.; Jeong, E.; Ko, J. *Anal. Sci.* **2004**, *20*, x155.
18. Hotta, S.; Goto, M. *Adv. Mater.* **2002**, *14*, 498.
19. Yassar, A.; Demanze, F.; Jaafari, A.; Idrissi, M. E.; Coupry, C. *Adv. Funct. Mater.* **2002**, *12*, 699.
20. Fichou, D. *J. Mater. Chem.* **2000**, *10*, 571.
21. Lee, C.; Kim, C.; Park, J. W. *J. Electroanal. Chem.* **1994**, *374*, 115.
22. Agrawal, A. K.; Jenekhe, S. A. *Chem. Mater.* **1996**, *8*, 579.
23. Peter, B.; Frank, W.; Gunther, G.; Franz, E. *Synthesis* **1993**, *11*, 1099.
24. Bruker. *SMART and SAINT: Area Detector Control and Integration Software Ver. 5.0*; Bruker Analytical X-ray Instruments: Madison, WI, 1998.
25. Bruker. *SHEXTL: Structure Determination Programs Ver. 5.16*; Bruker Analytical X-ray Instruments: Madison, WI, 1998.